

# Carrier-envelope phase effects for a dipolar molecule interacting with two-color pump-probe laser pulses

Taiwang Cheng and Alex Brown\*

*Department of Chemistry, University of Alberta, Edmonton, Alberta, Canada T6G 2G2*

(Received 28 June 2004; revised manuscript received 27 September 2004; published 17 December 2004)

The interaction of a two-level dipolar molecule with two laser pulses, where one laser's frequency is tuned to the energy level separation (pump laser) while the second laser's frequency is extremely small (probe laser), is investigated. A dipolar molecule is one with a nonzero difference between the permanent dipole moments of the molecular states. As shown previously [A. Brown, *Phys. Rev. A* **66**, 053404 (2002)], the final population transfer between the two levels exhibits a dependence on the carrier-envelope phase of the probe laser. Based on the rotating-wave approximation (RWA), an effective Hamiltonian is derived to account for the basic characteristics of the carrier-envelope phase dependence effect. By analysis of the effective Hamiltonian, scaling properties of the system are found with regard to field strengths, pulse durations, and frequencies. According to these scaling properties, the final-state population transfer can be controlled by varying the carrier-envelope phase of the probe laser field using lasers with weak field strengths (low intensities) and relatively long pulse durations. In order to examine the possible roles of background states, the investigation is extended to a three-level model. It is demonstrated that the carrier-envelope phase effect still persists in a well-defined manner even when neighboring energy levels are present. These results illustrate the potential of utilizing excitation in dipolar molecules as a means of measuring the carrier-envelope phase of a laser pulse or if one can manipulate the carrier envelope phase, as a method of controlling population transfer in dipolar molecules. The results also suggest that the carrier-envelope phases must be taken into account properly when performing calculations involving pump-probe excitation schemes with laser frequencies which differ widely in magnitude.

DOI: 10.1103/PhysRevA.70.063411

PACS number(s): 32.80.Qk, 33.80.Wz

## I. INTRODUCTION

In recent years, due to advances in laser technology, few-cycle (optical) laser pulses [1] have been widely used either to probe the properties of matter or to control the physical processes arising from the laser-matter interaction. For such short pulses, the timing of the field oscillation cycles within a laser pulse will play an important role. For example, for a few-cycle laser pulse, the time-dependent electric field  $E(t) = f(t)\cos(\omega t + \delta)$  will change significantly if the carrier-envelope phase (CEP)  $\delta$  of the pulse—i.e., the relative phase of the carrier frequency with respect to the pulse envelope  $f(t)$ —is changed. Note that the CEP is sometimes also referred to as the “absolute” phase.

The dependence of physical observables on the CEP is quite general for laser pulses of a few optical cycles interacting with matter. Both experimental and theoretical studies have revealed a variety of laser-induced processes that depend on the CEP of the laser field causing the excitation. The majority of these studies fall into three categories: angular distributions of photoelectrons emitted from atomic targets [2–14], high-harmonic generation [15–22], and photoemission yields from metal surfaces [23–25]. There have been fewer investigations of the use of few-cycle laser pulses with a well-defined CEP for inducing and controlling dynamics in molecular systems [26–29]. These studies have investigated the role of the CEP in the control of  $\text{HCN} \rightarrow \text{HNC}$  isomer-

ization [26], in the vibrational trapping of  $\text{HD}^+$  and  $\text{HCl}^+$  molecular ions [27], in the modification of the dissociation probabilities for  $\text{HOD}$  and  $\text{H}_2\text{O}$  [28], and in the control of transition probabilities in dipolar molecules [29]. As intuitively predicted, most of the investigations where dependence of observables on the CEP is exhibited have the requirement of ultrashort pulse duration such that only a few optical cycles are contained within the pulse envelope—e.g.,  $\approx 5$  fs for  $\lambda = 800$  nm. However, Sansone *et al.* [15] have recently demonstrated the CEP dependence of high-harmonic generation in Ar using 20-fs pulses with a wavelength of 800 nm. Additionally, in order for the CEP effects to manifest themselves, many of the proposed schemes, especially those involving atomic targets, require lasers of high intensity ( $> 10^{14}$  W/cm<sup>2</sup>). In general, the CEP dependence of photoemission from metals involves lasers of lower intensity—i.e.,  $I \approx 10^{12}$  W/cm<sup>2</sup>. While these requirements are true of most mechanisms involving a single pulsed laser, Brown and Meath have discussed [29] frequency and intensity scaling as it pertains to CEP effects. These scaling properties are apparent in experimental measurements of CEP effects involving excitation of atomic Rydberg states using much weaker radio-frequency fields [4,30]. Also, it should be emphasized that the importance of the CEP does not simply depend on how many laser cycles are contained within the pulse but rather depends on the rise and fall times of the pulse [27,29,30].

Recently, one of the authors (A.B.) and co-workers have proposed a two-laser pump-probe scenario that can be used to access the CEP of the probe laser [31,32]. Two other

\*Electronic address: alex.brown@ualberta.ca

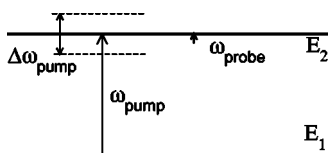


FIG. 1. Schematic of the two-level system interacting with pump ( $\omega_{\text{pump}} \approx E_{21}$ ) and probe lasers ( $\omega_{\text{probe}} \ll E_{21}$ ). The spectral bandwidth spanned by the temporally short pump pulses is indicated by  $\Delta\omega_{\text{pump}}$ .

multiple-pulse excitation schemes have also been proposed where a physical observable depends on the CEP of one of the laser fields [33,34]. These are distinct from the usual multipulse excitations which depend on the relative phase difference between the pulses [35,36]. Brumer, Frishman, and Shapiro [33] have predicted chiral selection, within a minimal four-level model of *L* and *D* enantiomers, that depends on the CEP of one laser in a three-laser excitation scheme. In a recent paper [34], which is similar in spirit to our pump-probe work in dipolar molecules [31,32], Bandrauk *et al.* have proposed a technique for measuring the CEP of a femtosecond infrared (IR) laser pulse with the help of an attosecond ultraviolet laser pulse. They demonstrated that the asymmetry in photoelectron signals from hydrogen atom excitation reproduced the electric field of the IR pulse. Thus, the ionization asymmetry could be used to measure directly the carrier-envelope phase of the femtosecond IR pulse.

In this paper, we primarily consider the interaction of a two-level dipolar ( $\vec{d} \neq 0$ ) molecule with two-color pump-probe laser pulses. The pump laser frequency is tuned close to the energy level separation of the stationary states ( $\omega_{\text{pump}} \approx E_{21} = E_2 - E_1$ ), and the probe laser frequency is much smaller compared to the energy level separation ( $\omega_{\text{probe}} \ll E_{21}$ ). The pulse duration of the pump pulse is chosen such that its spectral bandwidth is significant relative to the probe frequency. The terms “pump” and “probe” refer to the relative magnitude of the carrier frequencies of the pulses rather than to their time order. Figure 1 presents a schematic for the model system. For this system, obvious dependence of the final molecular state populations on the probe laser CEP has been determined [31,32], even for situations when the pump and probe laser pulses are several tens of optical periods long. It was shown [31,32] that the probe laser CEP effect is negligible for nondipolar ( $d=0$ ) molecules. In Sec. II, we develop analytic expressions based on the rotating-wave approximation (RWA) that allow the determination of the physical origin of the CEP effect. The expressions developed provide an interpretation of the strong CEP dependence of the excitation process as due to the interference of multiple optical paths from the initial to the final state or, alternatively, as due to the probe laser becoming an effective ultrashort pulse modulated by the pump pulse envelope. From the RWA Hamiltonian derived, scaling properties for the system are determined and show that a large CEP dependence can also be observed for long laser pulses with relatively weak field strengths. In Sec. III A, we demonstrate the applicability of the RWA expressions by comparing final excited-state populations calculated using the RWA to exact results.

While two-level models are extremely useful, the role of background states is investigated in Sec. III B by considering several three-level systems. The effect of the third level on the CEP dependence of the final excited-state populations is examined via exact calculations. Finally, in Sec. IV, we draw some brief conclusions regarding the utility of these results. Unless stated otherwise, atomic units are used throughout this paper.

## II. THEORY

Within the semiclassical dipole approximation, the time-dependent wave function for a *N*-level molecule interacting with an electric field (laser or lasers) is given in matrix form by

$$i \frac{\partial \underline{a}(t)}{\partial t} = \underline{H}(t) \underline{a}(t) = [\underline{E} - \underline{\vec{\mu}} \cdot \vec{\varepsilon}(t)] \underline{a}(t). \quad (1)$$

Here  $\underline{a}(t)$  is the column vector defined by  $[\underline{a}(t)]_j = a_j(t)$ , and the energy and dipole moment matrices are defined by  $(\underline{E})_{jk} = E_j \delta_{jk}$  and  $(\underline{\vec{\mu}})_{jk} = \langle \phi_j | \vec{\mu} | \phi_k \rangle$ , where  $\vec{\mu}$  is the dipole moment operator and  $\phi_j$  is the orthonormalized time-independent wave function for stationary state *j* having energy  $E_j$ . For a two-level model, as considered in Sec. III A, *j* and *k* run over the indices 1 and 2 while for the three-level model considered in Sec. III B, the indices run from 1 to 3. In Eq. (1),  $\vec{\varepsilon}(t)$  represents the total time-dependent electric field. For the pump-probe pulsed laser excitation process considered here, the electric field can be written as

$$\vec{\varepsilon}(t) = \sum_{i=1}^2 \hat{e}_i \varepsilon_i f_i(t) \cos(\omega_i t + \delta_i), \quad (2)$$

where  $\hat{e}_i$ ,  $\varepsilon_i$ ,  $\omega_i$ ,  $\delta_i$ , and  $f_i(t)$  are the polarization vector, amplitude, frequency, CEP, and pulse envelope of field *i*, respectively. The subscript 1 refers to the pump laser while 2 refers to the probe laser. The pulse envelopes considered are Gaussian,  $f_i(t) = \exp[-(t/\tau_i)^2]$ , where  $\tau_i$  is the pulse length for field *i*. The time delay between the two laser pulses is set to zero for simplicity; the effect of time delay is considered elsewhere [37]. Therefore, the terms “pump” and “probe” do not refer to the relative time order of the pulses but to the relative magnitudes of their carrier frequencies.

As is well known, generally, closed-form expressions are not available for the time-dependent state amplitudes  $a_j(t)$  in Eq. (1). Before we proceed further theoretically, we note that, numerically, the exact time-dependent amplitudes  $a_j(t)$  can be obtained by using the Crank-Nicholson method [38] to solve Eq. (1). For a small time step *dt*, over which the total electric field can be considered constant, the state amplitudes can be determined from

$$\underline{a}(t + dt) = \exp[-i \underline{H} dt] \underline{a}(t) \approx \left[ \frac{1 - i \underline{H} dt/2}{1 + i \underline{H} dt/2} \right] \underline{a}(t). \quad (3)$$

Repeatedly applying the above equation will generate the time evolution of the system, and the state populations can be determined via  $P_j(t) = |a_j(t)|^2$  using the appropriate initial conditions. Here the molecule is taken to be in the ground

state initially—i.e.,  $a_1(t_i)=1$  and  $a_n(t_i)=0$  ( $n \geq 2$ ) where  $t_i$  is the time that the laser-molecule interaction begins. The final-state populations will be  $P_j(t_f)$ , where  $t_f$  is the time that the laser-molecule interaction ends. While in general  $t_f \rightarrow \infty$  ( $t_i \rightarrow -\infty$ ) for Gaussian pulses, numerically we choose a final time  $t_f = \alpha\tau$  (an initial time  $t_i = -\alpha\tau$ ) such that the perturbation of the molecule by the field for  $|t| > \alpha\tau$  is negligible. Since  $\tau_{\text{probe}} > \tau_{\text{pump}}$  for the situations considered in this paper,  $\tau$  is the probe pulse duration. The numerical parameter  $\alpha=4$  for the Gaussian pulses considered in this paper.

We now proceed with an analytic derivation for the two-level model, which has been studied previously [31,32] for the excitation scheme given in Fig. 1. The approximate model developed below for two levels provides further insight into the physical processes leading to the probe laser carrier envelope phase effect and allows optimum conditions for exhibiting the effect to be determined. All results presented for the three-level model are determined exactly using Eq. (3).

For later theoretical simplicity, we transform from the  $q(t)$  representation into an interaction representation defined by

$$a_j(t) = b_j(t) \exp \left\{ -i \left[ E_j(t-t_i) - \vec{\mu}_{jj} \cdot \int_{t_i}^t \vec{\varepsilon}(t') dt' \right] \right\}. \quad (4)$$

The coefficients  $b_j(t)$  then satisfy

$$i \frac{d}{dt} \begin{pmatrix} b_1(t) \\ b_2(t) \end{pmatrix} = \begin{pmatrix} 0 & H_{12} \\ H_{21} & 0 \end{pmatrix} \begin{pmatrix} b_1(t) \\ b_2(t) \end{pmatrix}, \quad (5)$$

with the diagonal matrix elements of the Hamiltonian equal to zero and the off-diagonal matrix elements given by

$$H_{12} = H_{21}^* = -\vec{\mu}_{12} \cdot \vec{\varepsilon}(t) \exp \left[ -iE_{21}(t-t_i) + i\vec{d} \cdot \int_{t_i}^t \vec{\varepsilon}(t') dt' \right]. \quad (6)$$

Here we have introduced two important parameters to characterize the system: the energy separation of the excited and ground states,  $E_{21} = E_2 - E_1 > 0$ , and the difference between the permanent dipole moments of the excited and ground states,  $\vec{d} = \vec{\mu}_{22} - \vec{\mu}_{11}$ .

Up until this point, everything is general and exact for the two-level system. To simplify the problem, we assume that the lasers are linearly polarized and  $\vec{\mu}_{12} \parallel \vec{d} \parallel \vec{\varepsilon}(t)$ . Therefore, only the magnitudes of the dipole moments and laser fields will be indicated subsequently; the effect of orientational averaging is the subject of another paper [37].

Following Ref. [39], if the durations of the pulses,  $\tau_1$  and  $\tau_2$ , are long enough—i.e.,  $(\omega_1 \tau_1)^{-1} \ll 1$  and  $(\omega_2 \tau_2)^{-1} \ll 1$ —we can approximate  $H_{12}$  in Eq. (6) as

$$H_{12} = H_{21}^* = -\mu_{12} [\varepsilon_1 f_1(t) \cos(\omega_1 t + \delta_1) + \varepsilon_2 f_2(t) \cos(\omega_2 t + \delta_2)] \times \exp[-iE_{21}(t-t_i)] \exp\{i[z_1 f_1(t) \sin(\omega_1 t + \delta_1) + z_2 f_2(t) \sin(\omega_2 t + \delta_2)]\}, \quad (7)$$

where  $z_1 = \varepsilon_1 d / \omega_1$  and  $z_2 = \varepsilon_2 d / \omega_2$ . Using the identity

$$\exp[ix \sin(\theta)] = \sum_n J_n(x) \exp(in\theta) \quad (8)$$

and the recursion relation

$$J_n(x) = \frac{x}{2n} [J_{n-1}(x) + J_{n+1}(x)], \quad (9)$$

the off-diagonal matrix elements ( $H_{12} = H_{21}^*$ ) can be written as

$$H_{12} = -\frac{\mu_{12}}{d} \sum_{m=-\infty}^{\infty} \sum_{n=-\infty}^{\infty} J_m(z_1 f_1(t)) J_n(z_2 f_2(t)) (m\omega_1 + n\omega_2) \times \exp[-i(E_{21} - m\omega_1 - n\omega_2)t] \exp[i(m\delta_1 + n\delta_2)]. \quad (10)$$

In Eqs. (8)–(10),  $J_n(x)$  is a Bessel function of integer order  $n$  and argument  $x$ . The unimportant overall phase factor  $\exp(iE_{21}t)$  has been omitted from Eq. (10) for clarity.

For the frequencies we are considering,  $\omega_1 \approx E_{21}$  and  $\omega_2 \ll E_{21}$ , the dominant interactions will involve the absorption of a single photon of frequency  $\omega_1$ . Thus, we can set  $m=1$ . As long as the field strength of the pump laser is such that  $\mu_{12}\varepsilon_1/E_{21} \ll 1$ , the use of this RWA is justified; the RWA is not invoked for the probe laser field. The Hamiltonian matrix elements  $H_{12} = H_{21}^*$  can then be written as

$$H_{12} = -\frac{\mu_{12}\omega_1}{d} \exp(-i\Delta t) J_1(z_1 f_1(t)) \exp(i\delta_1) \times \left[ \sum_{n=-\infty}^{\infty} J_n(z_2 f_2(t)) \exp[in(\omega_2 t + \delta_2)] + \sum_{n=-\infty}^{\infty} \left( \frac{n\omega_2}{\omega_1} \right) J_n(z_2 f_2(t)) \exp[in(\omega_2 t + \delta_2)] \right]. \quad (11)$$

Here  $\Delta = E_{21} - \omega_1$  is the detuning from the one-photon resonance. The overall phase factor  $\exp(i\delta_1)$  could be omitted from Eq. (11). Therefore, it is clear from Eq. (11) that the final population transfer is independent of the pump laser's CEP  $\delta_1$ . Of course, this also implies that the final population transfer does not depend on the relative phase difference between the fields. Since the analytic expression indicates that the final results are independent of the pump laser's CEP, all exact calculations are carried out for  $\delta_1=0$ ; previous exact calculations [31] have verified the  $\delta_1$  independence of the final excited-state populations for the laser parameters considered in this paper.

When  $n$  is small,  $n\omega_2/\omega_1 \ll 1$  since  $\omega_2 \ll E_{21} \approx \omega_1$ . Therefore, for small  $n$ , the first term in the brackets of Eq. (11) will dominate the second term. On the other hand, when  $n$  becomes large, such that  $n\omega_2/\omega_1$  is greater than or equal to 1,  $J_n(z_2 f_2(t))$  becomes exponentially small, at least for the parameters considered in this paper where  $z_2 \leq 1$  [40]. Thus, the second term can be omitted again. So only the first term in the brackets of Eq. (11) is retained. Under this assumption, the Hamiltonian matrix elements are

$$H_{12} = H_{21}^* = -\frac{\mu_{12}\omega_1}{d} J_1(z_1 f_1(t)) \times \exp(-i\Delta t) \sum_{n=-\infty}^{\infty} J_n(z_2 f_2(t)) \exp[in(\omega_2 t + \delta_2)]. \quad (12)$$

By using Eq. (8), we can recontract the summation to obtain

$$H_{12} = -\frac{\mu_{12}\omega_1}{d} J_1(z_1 f_1(t)) \exp(-i\Delta t) \exp[iz_2 f_2(t) \sin(\omega_2 t + \delta_2)]. \quad (13)$$

From a practical viewpoint, usually a short pump pulse is interrogating the CEP of a longer probe pulse—i.e.,  $\tau_1 \ll \tau_2$ . Thus in the regime where  $z_1 f_1(t)$  is significant—i.e.,  $|t| < 4\tau_1$ — $f_2(t) \approx 1$  (see the discussion below for a quantitative example). Under these conditions, we reach an effective Hamiltonian to approximate the exact Hamiltonian of Eq. (6) as

$$H_{12} = -\frac{\mu_{12}\omega_1}{d} J_1(z_1 f_1(t)) \exp(-i\Delta t) \exp[iz_2 \sin(\omega_2 t + \delta_2)]. \quad (14)$$

Furthermore, if  $z_1 = d\varepsilon_1/\omega_1$  in Eq. (14) is small (note that for all the calculations in this paper,  $z_1 < 0.7$ ), then the expansion for the Bessel function,

$$J_1(zf(t)) = f(t) \sum_{n=0}^{\infty} \frac{\{z[1-f^2(t)]/2\}^n}{n!} J_{1+n}(z), \quad (15)$$

can be used and only the first term in the infinite summation can be retained. Thus,  $H_{12}$  in Eq. (14) can be approximated as

$$H_{12} = -\frac{1}{2}\mu_{12}\varepsilon_1 f_1(t) \exp(-i\Delta t) \exp[iz_2 \sin(\omega_2 t + \delta_2)]. \quad (16)$$

In obtaining Eq. (16), we have also made use of the fact that for  $z_1 < 0.7$ ,  $J_1(z_1)$  can be well approximated as  $z_1/2$  (note  $z_1 = \varepsilon_1 d/\omega_1$ ). Equation (16) is the basic result of this paper. When the pump pulse is tuned exactly to the one-photon resonance  $\Delta=0$ , scaling properties can be readily identified from Eq. (16). For a given set of molecular parameters ( $E_{21}$ ,  $\mu_{12}$ , and  $d$ ), if the field parameters are scaled by a parameter  $\gamma$  such that  $\omega_2 \rightarrow \omega_2/\gamma$ ,  $\varepsilon_2 \rightarrow \varepsilon_2/\gamma$ ,  $\varepsilon_1 \rightarrow \varepsilon_1/\gamma$ , and  $\tau_1 \rightarrow \gamma\tau_1$ , then Eq. (5) would be invariant under the Hamiltonian, Eq. (16). Because the validity of Eq. (16) depends on  $z_1 = d\varepsilon_1/\omega_1$  being small, the rescaling parameter should be considered to be greater than 1,  $\gamma > 1$ .

### A. Two-level model

First, we need to show that the effective Hamiltonian, Eq. (16), provides good agreement with the exact results in parameter regimes where all the approximations used in deriving it are justified. The model system and laser parameters we utilize come from recent studies [31,32] of the probe

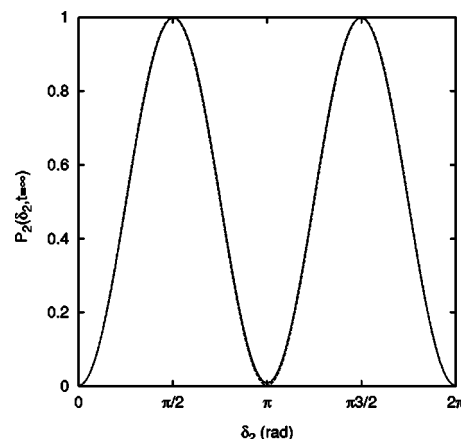


FIG. 2. The final population of the excited state  $P_2(\delta_2, \infty)$  versus probe laser CEP  $\delta_2$  for parameters described in text. The solid line is the exact result and the dashed line is the approximate result.

laser CEP effect. The two-level model is representative of a substituted aromatic molecule [41]. The relevant system properties are  $E_{21}=0.1$  a.u. ( $21\,947\text{ cm}^{-1}$ ),  $\mu_{12}=3.0$  a.u. ( $7.62\text{ D}$ ), and  $d=6.5$  a.u. ( $16.52\text{ D}$ ). The pump ( $i=1$ ) and probe ( $i=2$ ) laser parameters are  $\omega_1=E_{21}=0.1$  a.u.,  $\omega_2 = \omega_1/11$ ,  $\varepsilon_1=3.9 \times 10^{-3}$  a.u. ( $I=5.3 \times 10^{11}\text{ W/cm}^2$ ),  $\varepsilon_2=8.5 \times 10^{-4}$  a.u. ( $I=2.5 \times 10^{10}\text{ W/cm}^2$ ),  $\tau_1=15.2$  fs (10 optical cycles), and  $\tau_2=250$  fs (15 optical cycles). Using these parameters, all approximation made in reaching Eq. (16) are reasonable—i.e.,  $(\omega_1\tau_1)^{-1}=0.016 \ll 1$ ,  $(\omega_2\tau_2)^{-1}=0.011 \ll 1$ ,  $\mu_{12}\varepsilon_1/E_{21}=0.117 \ll 1$ ,  $z_1=d\varepsilon_1/\omega_1=0.25$ ,  $z_2=d\varepsilon_2/\omega_2=0.61 \ll \omega_1/\omega_2=11$ , and at  $|t|=4\tau_1$ ,  $f_2(t)=0.94 \approx 1$ . It is shown in [31] that for these parameters, complete control can be achieved by varying the probe laser carrier phase  $\delta_2$  from 0 to  $\pi/2$ ; i.e., the final excited-state population  $P_2(\delta_2, \infty) = |a_2(\delta_2, \infty)|^2$  changes from 0 to 1 over this CEP range. In Fig. 2, we compare the final excited-state population  $P_2(\delta_2, \infty)$  versus the CEP of the probe laser as determined from the exact Hamiltonian, Eq. (6), and from the approximate Hamiltonian, Eq. (16). For these choices of laser parameters, the approximate results are in good quantitative agreement with the exact ones. Two symmetries can be identified in Fig. 2—i.e.,  $P_2(\delta_2, \infty) = P_2(2\pi - \delta_2, \infty)$  and  $P_2(\delta_2, \infty) = P_2(\pi - \delta_2, \infty)$ . These can be readily explained using the approximate Hamiltonian, Eq. (16). From Eq. (16), we have  $H_{12}(-t, \delta_2) = H_{12}^*(t, 2\pi - \delta_2)$ . If we define  $U(t_i, t_f, \delta_2)$  as the evolution operator from  $t_i$  to  $t_f$  with CEP  $\delta_2$ , we have  $U(-\infty, \infty, \delta_2) = U^*(-\infty, \infty, 2\pi - \delta_2)$  and thus  $P_2(2\pi - \delta_2) = P_2(\delta_2)$ . For the special case where the pump laser is tuned exactly to the one-photon resonance ( $\Delta = E_{21} - \omega_1 = 0$ ), as in Fig. 2, we have  $H_{12}(-t, \delta_2) = H_{12}(t, \pi - \delta_2)$ . In this case,  $U \times (-\infty, \infty, \delta_2) = U(-\infty, \infty, \pi - \delta_2)$  and  $P_2(\pi - \delta_2) = P_2(\delta_2)$ . Due to these symmetries, we only consider the parameter regime of  $\delta_2 \in [0, \pi]$  for the following examples utilizing the two-level model.

We now consider a wider parameter space to further test the validity of Eq. (16). The parameter regime presented in Fig. 3 of Ref. [31], where  $\varepsilon_1 \in [0.002:0.01]$ ,  $\delta_2 \in [0, \pi]$ , and the other parameters are the same as for Fig. 2, is considered. Figure 3(a) illustrates the final excited-state population as

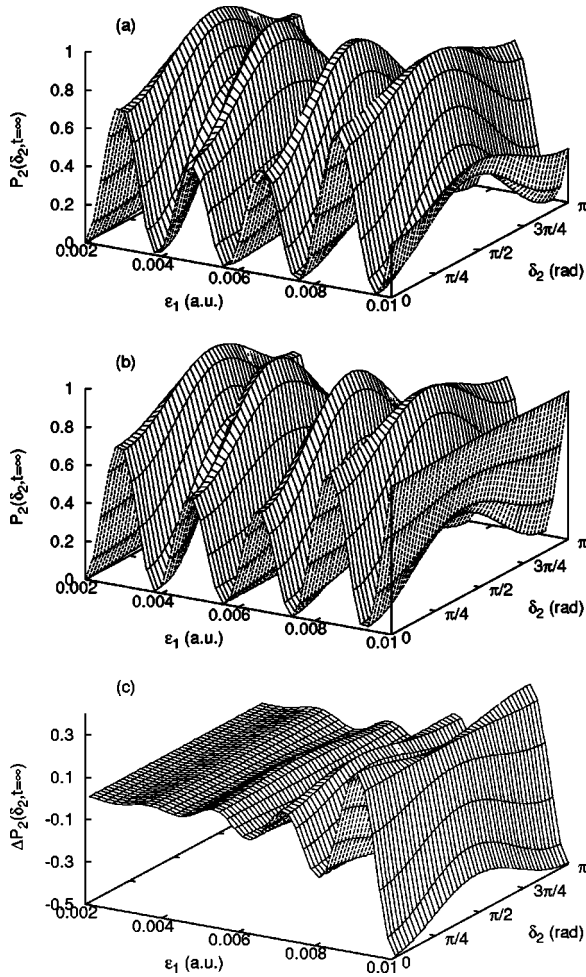


FIG. 3. The final population of the excited state  $P_2(\delta_2, \infty)$  versus probe laser CEP  $\delta_2$  and the pump laser field strength for (a) the exact results and (b) the approximate results. Panel (c) plots the difference between the exact and approximate results. See text for details.

determined from the exact Hamiltonian, Eq. (6), while Fig. 3(b) shows the results calculated using the approximate Hamiltonian, Eq. (16). The absolute difference between  $P_2(\delta_2, \infty)$  as determined from the exact and approximate Hamiltonians is plotted in Fig. 3(c). Comparing Figs. 3(a) and 3(b), the results are in excellent qualitative agreement. However, Fig. 3(c) reveals that there are significant quantitative discrepancies for  $\epsilon_1 > 0.005$  a.u. due to a systematic shift in the positions of maxima and minima; compare Figs. 3(a) and 3(b). For  $\epsilon_1 < 0.005$ , the results from Eq. (16) provide excellent quantitative agreement with the exact results; the absolute discrepancy of the final-state populations is less than 0.06.

We have also tested Eq. (16) for pump frequencies detuned from the one-photon resonance—i.e.,  $(E_{21} - \omega_1) = \Delta \neq 0$ . For these cases, the approximation also provides good agreement with the exact results (not shown here). Since the dependence of the final-state populations on the probe laser's CEP is strongest for the pump laser tuned exactly to the one-photon resonance [31], we concentrate on the  $\Delta = 0$  case in the following.

From Eq. (12), we can readily identify the origin of the CEP dependence effect since it provides a clear physical picture in the energy domain. As discussed in the original papers in [31,32] using an empirical model, the dependence of the final molecular-state population on the probe laser's CEP arises from the interference between different optical pathways from the initial to the final state. These pathways involve the same number of pump laser photons (here just one photon) but different numbers of probe photons. For example, we can include three possible optical pathways in Eq. (12) as has been done empirically in Refs. [31,32]; i.e., the number of pump and probe photons ( $N_{\text{pump}}, N_{\text{probe}}$ ) involved is (1,0), (1,1), and (1,-1). Including only these pathways and solving for the final-state population as a function of probe laser CEP phase, we obtain excellent quantitative agreement between these results and the exact results for the molecule and field parameters of Fig. 2.

By examining Eq. (16), we find a complementary physical picture for the CEP dependence in the time domain. In Eq. (16), the Hamiltonian takes the form of an “electric field”  $\exp[iz_2 \sin(\omega_2 t + \delta_2)]$  modulated by a “pulse envelope”  $f_1(t)$ . In order to have significant CEP dependence from this effective “laser pulse,” first  $z_2 = d\epsilon_2/\omega_2$  must not be too small, since for  $z_2 \ll 1$ ,  $\exp[iz_2 \sin(\omega_2 t + \delta_2)] \approx 1$  regardless of the value of  $\delta_2$ ; note that in the calculations presented here  $z_2 \sim 1$ . Second, if the optical period of the probe field is much greater than the pump pulse duration—i.e.,  $2\pi/\omega_2 \gg \tau_1$ —then  $z_2 \sin(\omega_2 t + \delta_2)$  will change little in the regime where  $f_1(t)$  is significant. Thus, there would be no phase dependence, as  $z_2 \sin(\omega_2 t + \delta_2)$  would become an overall phase factor that has no effect on the final-state populations. On the other hand, if the optical period of the probe laser is much smaller than pump pulse duration—i.e.,  $2\pi/\omega_2 \ll \tau_1$ —then there will be many effective “optical cycles” in the “pulse.” This situation is similar to that for a long pulse duration, where the CEP is not important. Clearly, for the pump-probe excitation scheme introduced in Refs. [31,32], it is not how many optical cycles are in the pump or probe laser pulses that is of critical importance. Rather, it is the number of probe optical cycles within the pump pulse that determines whether there is an effect of the CEP of the probe laser. This also explains why the probe pulse length does not affect the final phase dependence significantly as long as it contains several optical cycles. In fact, as is shown from Eqs. (13) and (14), a plane wave could be used to approximate the probe laser.

The above criteria suggest that the CEP dependence effect can be optimized (maximized) by choosing the pulse length of the pump laser  $\tau_1$  and the probe laser frequency  $\omega_2$  such that  $\omega_2 \sim 2\pi/\tau_1$ . Figure 4 illustrates the final excited-state population  $P_2(\delta_2, \infty)$  as a function of the probe laser's CEP and the pump laser's pulse length (which is given in units of optical period of pump laser,  $n_1 = \tau_1/[2\pi/\omega_1]$ ). Except for the change in the pulse length of the pump laser, all other molecular and laser parameters are the same as in Fig. 2. From Fig. 4, it is clear that the phase dependence is most significant for the pulse lengths where  $\omega_2 \sim 2\pi/\tau_1$ —i.e.,  $n_1 \sim \omega_1/\omega_2 = 11$ .

In Fig. 5, the dependence of final population of the excited state versus the probe laser CEP is presented for a

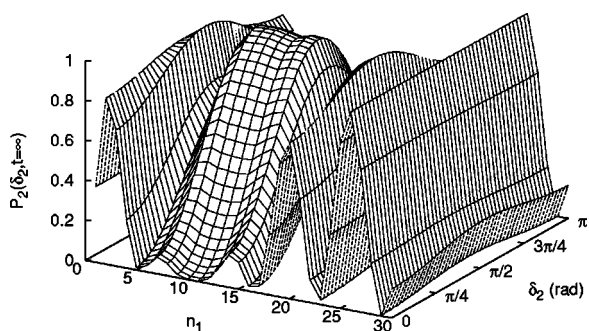


FIG. 4. The final population of the excited state  $P_2(\delta_2, \infty)$  versus probe laser CEP  $\delta_2$  and the duration of the pump laser (in units of optical period of pump laser; see text for details). Here we only show the exact numerical results.

rescaling of  $\gamma=10$ ; see the discussion in Sec. II. The laser parameters before rescaling are those of Fig. 2. With this scaling, the probe laser frequency is now 110 times smaller than the pump laser frequency,  $\omega_2=E_{21}/110$  ( $200 \text{ cm}^{-1}$ ). The field strength for the pump laser is  $3.9 \times 10^{-4}$  a.u. ( $I=5.3 \times 10^9 \text{ W/cm}^2$ ) and that for the probe laser is  $8.5 \times 10^{-5}$  a.u. ( $I=2.5 \times 10^8 \text{ W/cm}^2$ ). The pump pulse duration is 152 fs (100 optical cycles). The results presented in Fig. 5 have been determined by integrating Eq. (4) exactly. The complete phase control demonstrated in Fig. 2 is reproduced with the rescaled parameters. Therefore, complete phase control can be achieved for much weaker fields and longer pulse durations by using a low-frequency probe laser. Or thinking about the consequences in an alternative fashion, the dependence of the excited-state populations on CEP is manifested for weaker fields and longer pulse durations if the pump and probe frequencies differ greatly in magnitude—i.e.,  $\omega_1/\omega_2 \gg 1$ .

The significance of identifying scaling properties is that by using low-frequency pulses, much weaker fields may be used to detect the CEP dependence effect described in [31,32]. By utilizing weaker fields, alteration of the molecular system is minimized by excluding effects such as ioniza-

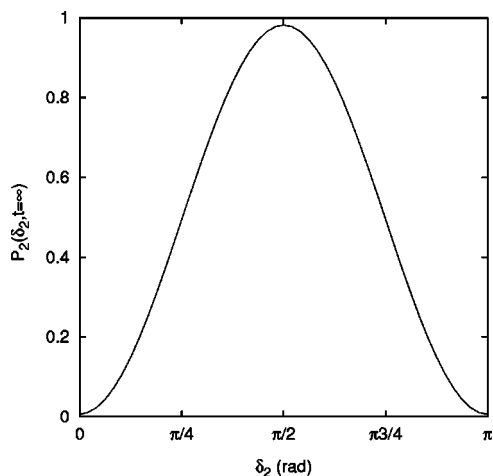


FIG. 5. The final population of the excited state versus probe laser CEP for the parameters in Fig. 2 rescaled by  $\gamma=10$  (see text for details).

tion and dynamic Stark energy level shifts. The two-level model is much more appropriate for weak fields and longer pulses [42] since the effects of background states are minimized. In addition, the use of a low-frequency laser makes it easier to stabilize and manipulate the probe laser phase [30]. Thus, experimental observation of the carrier-envelope phase dependence effect described here should be feasible.

### B. Three-level model

The two-level model clearly demonstrates the CEP dependence of the final-state populations for the excitation of dipolar molecules with the pump-probe scenario illustrated in Fig. 1. However, for molecular systems, the energy levels may be congested, and for a complex molecular system such as the one our two-level model is based upon, each of the two levels could be within a manifold of closely spaced energy levels. Between and within each manifold, the levels might be coupled by the probe laser frequency  $\omega_2$  and/or by the bandwidth of pump laser  $\Delta\omega_1 \sim 2\pi/\tau_1$ . In order to examine the role that background states may play in the expression of the CEP effect, we consider a three-level model. The general effects of background states can be extracted from this minimal model. It is again worth emphasizing the scalability of the CEP effect since reducing field strengths and increasing pulse durations will minimize the role of background states; i.e., the two-level model discussed in Sec. III A will be applicable.

We consider the effect of nearby levels by examining the same pump-probe excitation scheme given in Fig. 1 but for a three-level model, which is based on the previous two-level model. The pump ( $i=1$ ) and probe ( $i=2$ ) laser parameters are the same as those considered initially in Sec. III A—i.e.,  $\omega_1=E_{21}=0.1$  a.u.,  $\omega_2=\omega_1/11$ ,  $\epsilon_1=3.9 \times 10^{-3}$  a.u. ( $I=5.3 \times 10^{11} \text{ W/cm}^2$ ),  $\epsilon_2=8.5 \times 10^{-4}$  a.u. ( $I=2.5 \times 10^{10} \text{ W/cm}^2$ ),  $\tau_1=15.2$  fs (10 optical cycles), and  $\tau_2=250$  fs (15 optical cycles). The relevant system properties for levels 1 and 2 are  $E_{21}=0.1$  a.u. ( $21947 \text{ cm}^{-1}$ ),  $\mu_{12}=3$  a.u. (7.62 D), and  $d_{21}=\mu_{22}-u_{11}=6.5$  a.u. (16.52 D). A third energy level is introduced above the excited state. The important properties that define the third state are its energy spacing from the second state, the transition dipole connecting it to the ground state 1, the transition dipole connecting it to state 2, and its permanent dipole moment. The energy of the third state is chosen to be  $E_{31}=12E_{21}/11=E_{21}+\omega_2$ ,  $E_{31}=E_{21}+\omega_2/2$ , or  $E_{31}=E_{21}+2\omega_2$ . In the first case, levels 2 and 3 are exactly in resonance with the probe laser frequency  $\omega_2$ , and thus the sequential  $1 \rightarrow 2 \rightarrow 3$  excitation is feasible. In the second and third cases, levels 2 and 3 are off resonance and the third state may only be populated due to processes related to the bandwidth of the pump laser. Two possible situations are considered for the transition dipole moment connecting levels 1 and 3: one is for strongly coupled states—i.e.,  $\mu_{13}=1$ —and the other for uncoupled states—i.e.,  $\mu_{13}=0$ . For each of these  $1 \rightarrow 3$  transition dipole moments, three different transition dipole moments connecting states 2 and 3 have been considered:  $\mu_{23}=0.0$  a.u., 0.1 a.u., and 1.0 a.u. In order to ease interpretation, we consider the third level to have a permanent dipole moment such that  $d_{31}=\mu_{33}-\mu_{11}=6.5$  a.u.

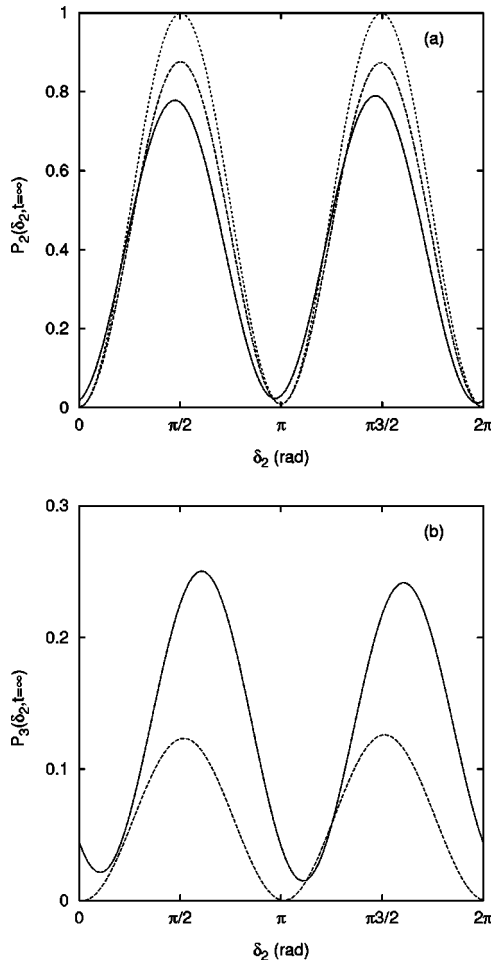


FIG. 6. The final population of the excited states versus probe laser CEP for the laser parameters of Fig. 2: (a) state 2 and (b) state 3. The transition dipole moment connecting states 2 and 3 is  $\mu_{23} = 1.0$  a.u. (solid line), 0.1 a.u. (dashed line), and 0.0 a.u. (dotted line). There is no transition dipole moment connecting states 1 and 3—i.e.,  $\mu_{13} = 0.0$  a.u. The final population of state 3 is zero when  $\mu_{13} = \mu_{23} = 0$  since this corresponds to the original two-level results of Fig. 2.

and  $d_{32} = \mu_{33} - \mu_{22} = 0$ . All of these molecular parameters are chosen to be realistic and to simulate the relevant effects of neighboring energy levels on the CEP dependence of the final excited-state populations in the  $1 \rightarrow 2$  transition.

We first consider the situation where states 1 and 3 are not coupled,  $\mu_{13} = 0$ , and the energy of the third state is chosen to be  $E_{31} = 12E_{21}/11 = E_{21} + \omega_2$ . Therefore, the population in the neighboring energy level 3 can only arise via sequential coupling through excited state 2. In Fig. 6, the final excited-state populations  $P_2(\delta_2, \infty)$  and  $P_3(\delta_2, \infty)$  are illustrated as a function of the probe laser's CEP for three choices of  $\mu_{23}$  (0 a.u., 0.1 a.u., and 1.0 a.u.). Note that  $\mu_{13} = 0$  plus  $\mu_{23} = 0$  corresponds to the original two-level results of Fig. 2 and thus the final population of state 3 is zero; see Fig. 6(b). The primary effect of the introduction of the third level is to cause a systematic decrease in the population of state 2. The CEP dependence of the final-state populations is retained and it has approximately the same symmetry as in the two-level case. There is a slight breaking of the symmetry—i.e.,

$P_2(\delta_2, \infty) \neq P_2(2\pi - \delta_2, \infty)$ —for the strongly coupled case where  $\mu_{23} = 1$ . The effect of the third level can be understood by considering the Rabi frequency of the population transfer from state 2 to state 3. Due to the sequentially coupled nature for this case, population in state 3 only arises via state 2. The Rabi period of the 2-3 transition,  $T \approx 2\pi/(\mu_{23}\epsilon_2)$ , is 1800 fs or 180 fs for  $\mu_{23} = 0.1$  or 1.0, respectively [note that  $f_2(t)$  is approximately constant during the pump pulse]. Since this Rabi period is much larger than the pump pulse length, the evolution of the system can be divided into two stages. In the first stage, the two-level system comprised of states 1 and 2 interacts with the pump and probe laser fields, and this results in the population of state 2 over a time scale dictated by the duration of the pump laser (which is much shorter than the Rabi period governing evolution into state 3). In the second stage, the two-level system comprised of states 2 and 3 interacts with only the probe laser as the pump laser has finished. As discussed in Sec. II, the first process depends on the CEP  $\delta_2$ . The second process which involves a weak laser field of long pulse duration is independent of  $\delta_2$ . Therefore, the behavior of this sequential coupled three-level system retains the general CEP dependence exhibited in the original two-level system. Note that as the Rabi period for the  $2 \rightarrow 3$  transition becomes shorter—i.e.,  $\mu_{23}$  increases for a fixed probe field strength—the excitation cannot be separated into these two sequential processes and the symmetry seen in the two-level system is broken.

We now consider the situation where state 3 is coupled directly to state 1 and, possibly, also to state 2. Again, the energy of the third state is chosen to be  $E_{31} = 12E_{21}/11 = E_{21} + \omega_2$ . Therefore, population in state 3 can arise both by direct excitation from state 1 and by sequential excitations via state 2. Figure 7 illustrates the final excited-state populations  $P_2(\delta_2, \infty)$  and  $P_3(\delta_2, \infty)$  as a function of the probe laser's CEP for three choices of  $\mu_{23}$  (0.0 a.u., 0.1 a.u., and 1.0 a.u.). Clearly, there is still a dependence of the final-state populations on the probe laser's CEP. The general phase dependence in the two-level system is retained for state 2 in the three-level system. However, the  $1 \rightarrow 3$  coupling introduces significant asymmetry in the final population of state 2 for the probe laser's CEP between  $[0, \pi]$  and  $[\pi, 2\pi]$ . The asymmetry arises since there is now a direct pathway from the ground state to excited state 3. The pump laser is not tuned to the one-photon resonance with state 3—i.e.,  $\omega_1 \neq E_{31}$ . As shown by Brown [31], for the two-level system, when the pump laser is tuned away from the one-photon resonance, there is symmetry around  $\delta_2 = \pi$  rather than around  $\pi/2$  as is the case here when the pump laser is tuned to the one-photon resonance. The broken symmetry in the three-level model arises due to competition between the direct excitation to state 3 versus excitation to state 2. It is thus dictated by the relative magnitudes of the  $\mu_{12}$  and  $\mu_{13}$  transition dipole moments and the pump laser field strength; recall that  $d_{12} = d_{13}$ , so the permanent dipole moments play no role in the competition between these two processes.

It should be emphasized that the results of Figs. 6 and 7 correspond to the worst case scenario, where the upper levels are resonantly coupled by  $\omega_2$  and state 3 is within the bandwidth of pump laser. Even for this case, the general CEP

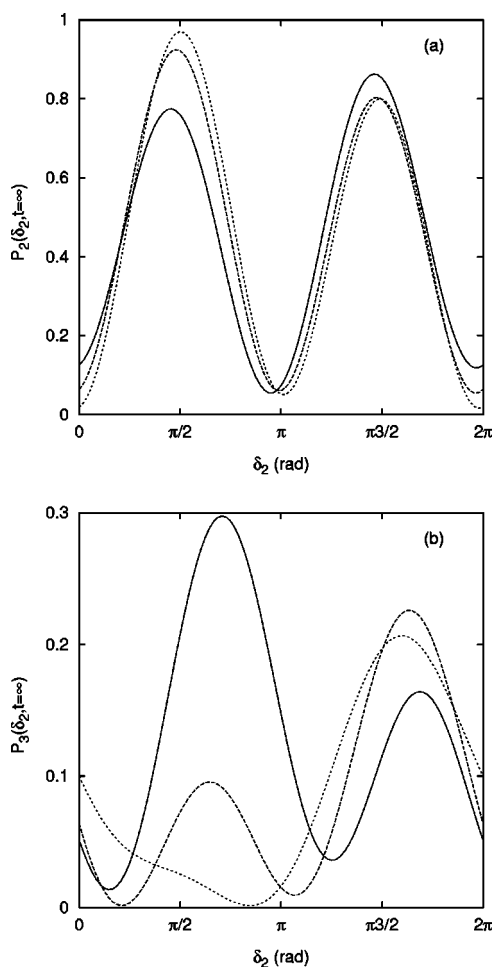


FIG. 7. The final population of the excited states versus probe laser CEP for the laser parameters of Fig. 2: (a) state 2 and (b) state 3. The transition dipole moment connecting states 2 and 3 is  $\mu_{23} = 1.0$  a.u. (solid line), 0.1 a.u. (dashed line), and 0.0 a.u. (dotted line). The transition dipole moment connecting states 1 and 3 is  $\mu_{13} = 1.0$  a.u.

dependence is well retained. However, due to the scaling law discussed in Sec. II, the original in-resonance system can always be rescaled to be off resonance. For example, for the above three-level system, if the molecular configuration is kept unchanged, but all the laser parameters are rescaled by  $\gamma=2$ , the resulting excitation probabilities to state 2 will return to the original two-level results shown in Fig. 2; i.e., the background level will have no effect.

We now explicitly consider the off-resonance case where the energy of the third state is chosen to be  $E_{31} = E_{21} + \omega_2/2$  or  $E_{31} = E_{21} + 2\omega_2$ . State 3 is coupled directly to state 1,  $\mu_{13} = 1.0$  a.u., and to state 2,  $\mu_{23} = 1.0$  a.u. Figure 8 illustrates the final excited-state populations  $P_2(\delta_2, \infty)$  and  $P_3(\delta_2, \infty)$  as a function of the probe laser's CEP for the two possible energies of state 3. As discussed above, the laser parameters are the same as for the results illustrated in Fig. 2. When state 3 is far off resonance of the probe laser frequency and outside the bandwidth of the pump laser—i.e.,  $E_{31} = E_{21} + 2\omega_2$ —the results are nearly identical to those for the two-level model; there is a very small population ( $<0.01$ ) in state 3. On the other hand, when state 3 is off resonance with the probe

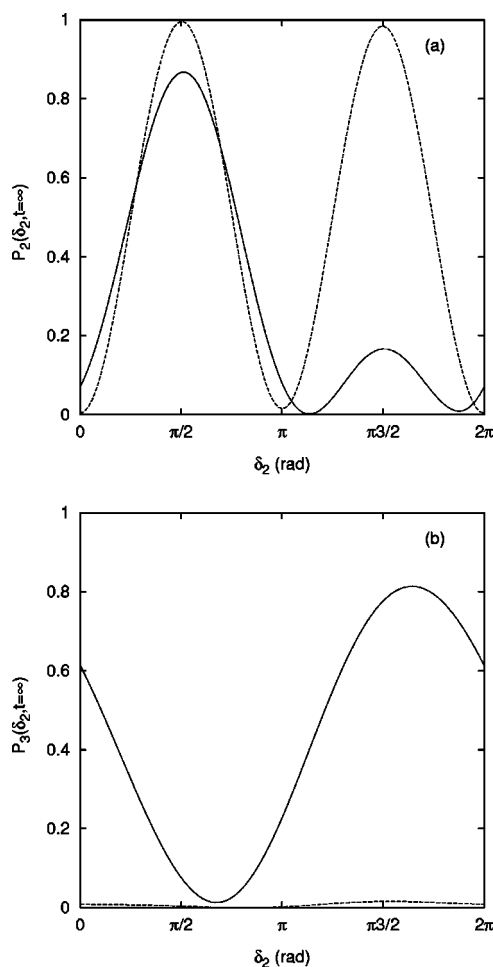


FIG. 8. The final population of the excited states versus probe laser CEP for the laser parameters of Fig. 2: (a) state 2 and (b) state 3. The transition dipole moment connecting states 2 and 3 is  $\mu_{23} = 1.0$  a.u. and the transition dipole moment connecting states 1 and 3 is  $\mu_{13} = 1.0$  a.u. The energy of the third state is  $E_{31} = E_{21} + \omega_2/2$  (solid line) or  $E_{31} = E_{21} + 2\omega_2$  (dashed line).

frequency but within the band width of the pump laser—i.e.,  $E_{31} = E_{21} + \omega_2/2$ —a significant asymmetry in the final population of state 2 for the probe laser's CEP between  $[0, \pi]$  and  $[\pi, 2\pi]$  is exhibited. As discussed for Fig. 7, the broken symmetry arises due to competition between the direct excitation to state 3 versus excitation to state 2. Clearly, if the probe laser is off resonance relative to the energy spacing with the background state and the bandwidth of the pump laser is smaller than the energy spacing, the two-level model becomes applicable. Both of these criteria can be satisfied utilizing the scaling rules that have been determined.

The results based on the three-level model demonstrate that the two-level model provides qualitatively correct behavior. While neighboring energy levels can influence the details of the CEP effect, it is important to note that the laser parameters can always be rescaled to quantitatively justify the use of a two-level model.

#### IV. SUMMARY AND CONCLUSIONS

By considering the Hamiltonians derived in Sec. II—i.e., Eqs. (12) and (16)—several important points with regards to

the appearance of the CEP effect in the two-level system can be noted. If the probe laser frequency is decreased, the pump pulse length must be increased for a CEP effect to be demonstrated in order to maintain the condition  $\tau_1 \approx 1/\omega_2$ . As the frequency of probe laser decreases, absorption pathways involving greater numbers of probe photons would be activated if the pump and probe laser field strengths are not adjusted accordingly; see Eq. (12). In general, having more active optical paths will decrease the dependence of the final molecular-state populations on the CEP of the probe laser [31]. If the pump and probe laser field strengths are decreased according to the rescaling of the parameters discussed in Sec. II, the laser plus molecule system will have the same physical conditions as the original one. Thus, for these scaled pulse parameters, an identical CEP dependence effect would be found as in the original situation. If there is strong CEP dependence of the final molecular-state populations in the original parameter regime, a much longer pump pulse length and much weaker fields could be used to achieve the same phase dependence which originally need relatively short pulses and strong fields.

If the carrier envelope phase of the probe pulse is unknown, the results presented here demonstrate that a second laser (the pump pulse) can be used to determine the CEP through a measurement of the excited-state population in dipolar molecules—e.g., as achieved through a subsequent ionization step and measurement of total ion yield. However, the measurement of an unknown carrier envelope phase requires detailed knowledge of the molecular structure—i.e., energies, transition dipole moments, and permanent dipole moments. Also, in the situations where the two-level results are most applicable—i.e., long and weak laser pulses where the scaling can be utilized—there is little need for measurement of the CEP since it can be measured via other means [30].

On the other hand, if the CEP of the probe laser can be precisely manipulated, the results presented here demonstrate that the final population of the excited state can be completely controlled—i.e., varied between 0% and 100% population. While this is certainly interesting, work is currently underway to determine if one can exhibit similar control, for example, in three-level systems where the upper levels are degenerate. This represents the simplest model for chemical control as the two degenerate states can correspond to different products.

The results presented here, as well as those in Refs. [31,32], also demonstrate that when a laser-matter interaction involving a temporally short high-frequency pump component (which leads to a resonance transition of the system) and a long low-frequency probe component is considered, the possible effects of the CEP must be examined carefully. The focus of this paper, as well as the previous ones [31,32], has been on situations where the CEP of the probe laser can be controlled. However, if the CEP of the laser pulses cannot be precisely controlled in experiments, the results clearly demonstrate that theoretical predictions must be properly phase averaged in order to interpret the experimental results. For example, if both carrier-envelope phases were set to zero (as is often done for calculations), when computing the final excited-state population for the molecule and field parameters of Fig. 2, a final-state population of zero would be predicted. However, if the properly phase-averaged results were determined, one would obtain  $P_2(\infty)=0.502$ .

In conclusion, we have further discussed the problem of using pump (in resonance with the two-level system) and probe (having a much smaller frequency than the energy level spacing) lasers to produce a CEP dependence of the final molecular-state populations in a simple two-level dipolar molecule. By considering a three-level model, we have shown that the CEP effect persists even in the presence of background states. Using RWA techniques, an effective Hamiltonian was derived for the two-level model that provides a clear physical picture of the CEP dependence effect from both the energy-domain and time-domain perspectives. In the energy domain, different photoexcitation channels interfere, while in the time domain, an effective ultrashort pulse is formed by the combination of pump and probe lasers. We demonstrated that the phase dependence will be most significant when the probe frequency is similar to the pulse duration of the pump laser—i.e.,  $\omega_2 \approx 2\pi/\tau_1$ . With the help of a qualitative discussion of the physical mechanism, scaling properties were found which show that using weak and low-frequency fields, a strong CEP dependence of the final molecular-state populations can still be exhibited. By rescaling the laser parameters, the effects of background states can be minimized or removed entirely. These findings may help the possible setup of experimental tests of the phase dependence effect described here.

- 
- [1] T. Brabec and F. Krausz, *Rev. Mod. Phys.* **72**, 545 (2000).  
 [2] X. Liu and C. Figueira de Morisson Faria, *Phys. Rev. Lett.* **92**, 133006 (2004).  
 [3] J. Zhang, X. Feng, Z. Xu, and D. S. Guo, *Phys. Rev. A* **69**, 043409 (2004).  
 [4] A. Gürtler, F. Robicheaux, W. J. van der Zande, and L. D. Noordam, *Phys. Rev. Lett.* **92**, 033002 (2004).  
 [5] J. Zhang and Z. Xu, *Phys. Rev. A* **68**, 013402 (2003).  
 [6] S. X. Hu and A. F. Starace, *Phys. Rev. A* **68**, 043407 (2003).  
 [7] D. B. Milosevic, G. G. Paulus, and W. Becker, *Opt. Express* **11**, 1418 (2003).  
 [8] G. G. Paulus, F. Grasbon, H. Walther, P. Villorresi, M. Nisoli, S. Stagira, E. Priori, and S. DeSilvestri, *Nature (London)* **414**, 182 (2001).  
 [9] D. B. Milosevic, G. G. Paulus, and W. Becker, *Phys. Rev. Lett.* **89**, 153001 (2002).  
 [10] S. Chelkowski and A. D. Bandrauk, *Phys. Rev. A* **65**, 061802(R) (2002).  
 [11] M. Kakehata, Y. Kobayashi, H. Takada, and K. Torizuka, *Opt. Lett.* **27**, 1247 (2002).  
 [12] P. Dietrich, F. Krausz, and P. B. Corkum, *Opt. Lett.* **25**, 16 (2000).

- [13] I. P. Christov, *Appl. Phys. B: Lasers Opt.* **70**, 459 (2000).
- [14] I. P. Christov, *Opt. Lett.* **24**, 1425 (1999).
- [15] G. Sansone, C. Vozzi, S. Stagira, M. Pascolini, L. Poletto, P. Villorosi, G. Tondello, S. DeSilvestri, and M. Nisoli, *Phys. Rev. Lett.* **92**, 113904 (2004).
- [16] A. Baltuška *et al.*, *Nature (London)* **421**, 611 (2003).
- [17] M. Nisoli, G. Sansone, S. Stagira, S. DeSilvestri, C. Vozzi, M. Pascolini, L. Poletto, P. Villorosi, and G. Tondello, *Phys. Rev. Lett.* **91**, 213905 (2003).
- [18] V. S. Yakovlev and A. Scrinzi, *Phys. Rev. Lett.* **91**, 153901 (2003).
- [19] R. M. Potvliege, N. J. Kylstra, and C. J. Joachain, *J. Phys. B* **33**, L743 (2000).
- [20] C. G. Durfee III, A. R. Rundquist, S. Backus, C. Herne, M. M. Murnane, and H. C. Kapteyn, *Phys. Rev. Lett.* **83**, 2187 (1999).
- [21] A. de Bohan, P. Antoine, D. B. Milošević, and B. Piraux, *Phys. Rev. Lett.* **81**, 1837 (1998).
- [22] P. Salières, P. Antoine, A. de Bohan, and M. Lewenstein, *Phys. Rev. Lett.* **81**, 5544 (1998).
- [23] P. Dombi, A. Apolonski, C. Lemell, G. G. Paulus, M. Kakehata, R. Holzwarth, T. Udem, K. Torizuka, J. Burgdörfer, and F. Krausz, *New J. Phys.* **6**, 39 (2004).
- [24] A. Apolonski *et al.*, *Phys. Rev. Lett.* **92**, 073902 (2004).
- [25] C. Lemell, X. M. Tong, F. Krausz, and J. Burgdörfer, *Phys. Rev. Lett.* **90**, 076403 (2004).
- [26] C. Uiberacker and W. Jakubetz, *J. Chem. Phys.* **120**, 11532 (2004).
- [27] H. Abou-Rachid, T. T. Nguyen-Dang, and O. Atabek, *J. Chem. Phys.* **110**, 4737 (1999).
- [28] M. V. Korolkov, J. Manz, and G. K. Paramonov, *Chem. Phys.* **217**, 341 (1997).
- [29] A. Brown and W. J. Meath, *J. Chem. Phys.* **109**, 9351 (1998).
- [30] W. M. Griffith, M. W. Noel, and T. F. Gallagher, *Phys. Rev. A* **57**, 3698 (1998).
- [31] A. Brown, *Phys. Rev. A* **66**, 053404 (2002).
- [32] A. Brown, W. J. Meath, and A. E. Kondo, *Phys. Rev. A* **65**, 060702(R) (2002).
- [33] P. Brumer, E. Frishman, and M. Shapiro, *Phys. Rev. A* **65**, 015401 (2002).
- [34] A. D. Bandrauk, S. Chelkowski, and N. H. Shon, *Phys. Rev. Lett.* **89**, 283903 (2002).
- [35] M. Shapiro and P. Brumer, *Adv. At., Mol., Opt. Phys.* **42**, 287 (2000).
- [36] R. J. Gordon and S. A. Rice, *Annu. Rev. Phys. Chem.* **48**, 601 (1997).
- [37] A. Brown, W. J. Meath, and A. E. Kondo (unpublished).
- [38] S. E. Koonin, *Computational Physics* (Benjamin-Cummings, Menlo Park, CA, 1986).
- [39] A. Brown, W. J. Meath, and P. Tran, *Phys. Rev. A* **65**, 063401 (2002).
- [40] S. Zhang and J. Jin, *Computation of Special Functions* (Wiley, New York, 1996).
- [41] W. Liptay, in *Excited States*, edited by E. C. Lim (Academic Press, New York, 1974), p. 198.
- [42] J. Cheng and J. Zhou, *Phys. Rev. A* **67**, 041404(R) (2003).